P.C. Chu and J.C. Gascard (Editors), *Deep Convection and Deep Water Formation in the Oceans.*

Forced Convection in the Upper Ocean near Fram Strait in Late Winter

Miles G. McPhee
McPhee Research Company
Naches, WA 98937 USA

ABSTRACT

Measurements of mean flow and turbulence in the boundary layer under drifting Arctic pack ice during the 1989 CEAREX O Camp experiment support the hypothesis that turbulence derived from internal waves and other flow features in the underlying pycnocline was an important factor in maintaining a deep mixed layer. Turbulent stress measurements in the upper 30 m of the boundary layer showed less attenuation with depth than previous experiments, implying existence of a source of turbulence in addition to shear at the ice/ocean interface. Although wind is usually the main source of shear between ice and ocean in the Arctic, in the O Camp region it was secondary to tidal currents apparently amplified by interaction with the Yermak Plateau. A packet of energetic internal waves impinging on the mixed layer/pycnocline interface at about 100 m depth is investigated, and appears to lose much of its energy to smaller scale motion there. It is suggested that similar phenomena may help account for the relative depth of the mixed layer in the central Weddell Sea, where deep convection has occurred in the past.

1. Introduction

Away from the continental slopes and marginal seas, the upper Arctic Ocean typically exhibits a strong pycnocline overlain by a relatively fresh mixed layer less than 60 m thick. The upper part of the pycnocline is cold, often near freezing, and strongly stratified by salinity; thus a very effective barrier exists between turbulent processes at the air-ice-sea interface and the warm Atlantic water at depth, and there is little possibility of deep convection and "catastrophic" overturn. The perennial ice pack in the Arctic provides a strong negative feedback to enhanced oceanic heat flux by its stabilizing effect on the boundary layer. In the Antarctic, the situation is different. Recent wintertime expeditions to the Weddell Sea (see, e.g., Gordon and Huber, 1990) have shown that the mixed layer there is relatively deep (>100 m) and stability is marginal. Martinson (1990; this volume) demonstrates that minor changes in a few key variables could nudge the present day Weddell into overturn, and the presence of a vast, all season polynya (the Weddell Polynya) during the 1970s shows that, once established, deep convection can apparently persist for years.

One of the more puzzling aspects of deep mixed layers in ice covered water is what keeps them mixed. The picture emerging from recent winter Antarctic work (Gordon and Huber, 1990) is one in which ice grows rapidly during the first few weeks of winter until it reaches a thickness of about 60 cm, after which heat conducted through the ice is roughly balanced by upward heat flux at the base of the mixed layer, and to first order, the system approaches a steady state with an upward heat flux estimated to be around 40 W m^{-2}. This is at least an order of magnitude larger than oceanic heat flux typically found under multi-year Arctic ice during the winter (McPhee and Untersteiner, 1982), but still much smaller than heat lost by open water in direct contact with the polar atmosphere. In terms of ocean boundary layer (OBL) physics, there is an important distinction between heat lost through conduction and heat lost directly to freezing. The thermal expansion coefficient is so small at temperatures near freezing that surface buoyancy flux is controlled almost exclusively by salinity, thus freezing produces a strong destabilizing buoyancy flux while heat loss through conduction has little effect on stability.

When forced convection at the surface is aided by destabilizing buoyancy flux, either from strong surface cooling in the open ocean, or from rapid ice growth when the mixed layer is at freezing, deep mixing is expected. However, when surface cooling is not accompanied by buoyancy flux, two factors work to limit the depth of mixing in polar boundary layers: (1) Coriolis attenuation of surface driven turbulent stress is large at high latitudes, consequently shear production of turbulent kinetic energy (TKE) falls off more rapidly and the rotational length scale (Ekman depth) for the boundary layer is smaller than at lower latitudes (an extreme example is presented by McPhee [1990, Fig. 6.9] where much of the stress attenuation and rotation occurs in the upper 10 m beneath a hydraulically smooth surface). (2) Processes that transport heat and salt into the boundary layer from below (the most likely candidates are direct upwelling and turbulent diffusion) also tend to reduce mixed layer depth, unless there is active entrainment at the top of the pycnocline.

During the *Coordinated Eastern Arctic Experiment* (CEAREX) *Oceanography Camp (*O Camp*)* drift in March and April of 1989, we encountered conditions that may bear on the question of what maintains deep, ice-covered mixed layers. In the region where the ice camp drifted (a southwest trajectory, centered at about 82^{o}30' N, 8^{o} E) the mixed layer was atypical of the Arctic in that it was salty (typically 34.1 psu), often about 100 m thick, and the halocline and thermocline coincided, so that the underlying warm (Atlantic) water was potentially in direct contact with the ice-covered surface. Since the ice cover was relatively compact and thick, convection driven by brine rejection was minor. The O Camp mixed layer was thus similar in some respects to the "cold" Weddell regime of Gordon and Huber (1990, see their Fig. 7c) except that the change in density across the pycnocline separating the mixed layer from the warm layer below was about twice as large in the Arctic, and the vertical extent of the pycnocline was much greater.

The intent of this paper is to explore characteristics of turbulence and other high frequency motions measured in the upper ocean under O Camp. Previous observations of turbulence under pack ice have underlined the importance of wind forcing: when the winds stops blowing, the ice/ocean shear and associated turbulence vanish. It is tempting to assume that the turbulent OBL set up by wind-driven drift across a quiescent ocean is similar to the OBL that would occur if the ocean flowed past stationary ice with the opposite velocity— this is the basis, e.g., of comparing the under-ice OBL with the atmospheric boundary layer (McPhee and Smith, 1976). The tacit assumption is that the only source of turbulence is shear at the ice-ocean interface. During much of the drift of O Camp we experienced strong diurnal currents relative to the ice that had little if any direct relation to the wind. The O Camp results suggest instead that turbulence generated by internal wave breaking near the mixed layer/pycnocline interface may have boosted overall turbulence levels in the mixed layer, and helped keep the mixed layer deep.

2. Turbulence Measurements

During O Camp, we deployed two instrument systems for measuring both mean and high frequency flow characteristics, using "turbulence clusters" (TC's) comprising three small current meters mounted along orthogonal axes near a Sea-Bird temperature/conductivity pair. The first system consisted of two rigid masts suspended through hydroholes with TC's at several levels down to 12 m below the ice, i.e., the upper part of the OBL. The second system (Fig. 1), newly developed for the O Camp experiment, is a rigid frame with 6 TC's spanning 11 m in the vertical, all interfaced to a Sea-Bird CTD unit equipped with compass and tiltmeters. Over the course of the experiment, the topmost cluster was eliminated, and one of the remaining temperature sensors failed, leaving 5 velocity turbulence clusters, with 4 including temperature and salinity. The whole "super CTD" can be lowered by a small winch to depths of 100 m or more. This system was intended mainly for studying internal waves and other small scale motions in the upper part of the pycnocline, but could also be positioned for boundary layer measurements nearer the surface.

From late on April 11, 1989 (day 101) through April 14 (day 104) a small storm was observed at O Camp with sustained easterly winds of 6-8 m/s (Guest and Davidson, 1989). For part of that period, the mobile CTVD frame was raised so that its topmost cluster was at approximately the same depth as the lowest cluster on the fixed mast, i.e., 12 m below the depth of the ice/ocean interface at 2.4 m. This provided a comparison between two clusters separated horizontally by about 6 m, and extended the turbulence measurements 9 m deeper in the boundary layer.

Turbulence statistics were extracted from the raw data as follows. The system samples velocity of each rotor six times per second, with these samples averaged for 1 s in the interface deck units and recorded digitally. For each cluster, sums of the data and data products and cross products are accumulated for 15 min periods, from which average velocities and zero lag covariances are calculated. Components of the Reynolds stress tensor are defined by

$$\tau_{ij} \equiv \langle (u_i - U_i)\ (u_j - U_j) \rangle$$

where angle brackets denote the ensemble spatial average, u_i is the instantaneous velocity component in the ith direction, and $U_i = \langle u_i \rangle$,. The true Reynolds stress is approximated by the covariance matrix under the assumption that a horizontally homogeneous field is advected past the probes in a steady flow. Obviously, these conditions are rarely encountered in nature, and our hope is that there is a "spectral gap" between the frequencies of the dominant turbulent eddies and other flow features. We have found from past measurements in the OBL (McPhee and Smith, 1976; McPhee, et. al, 1987) that an averaging interval of 15-20 minutes represents a suitable compromise between sampling the entire turbulent spectrum and having lower frequency, nonturbulent flow variations contaminate the statistics. Since the time scale of the most energetic turbulence eddies is of order minutes, there is much variability from one 15-min realization to another, especially in the off-diagonal (shear stress) components of the Reynolds stress tensor. Thus several 15-min realizations must

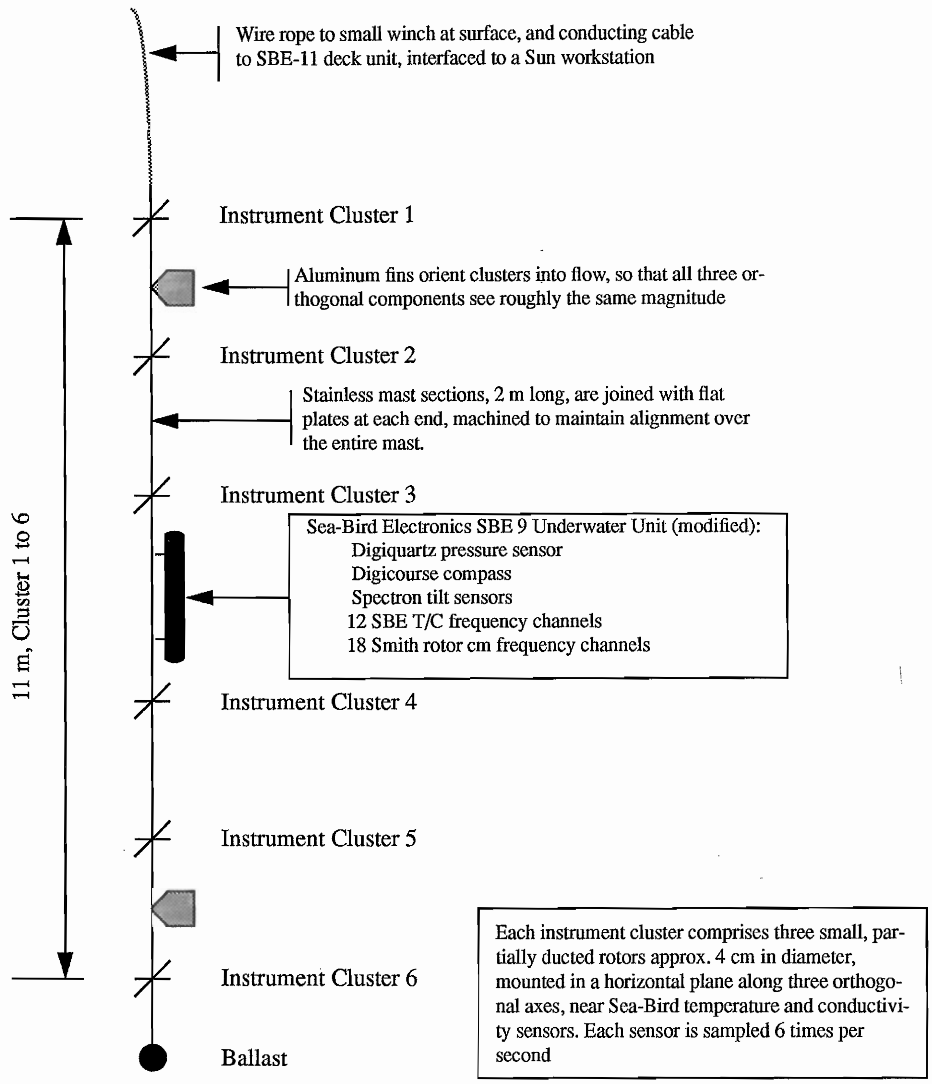

A Multi-level CTDV System on a Rigid Mast

Fig. 1. Schematic of the mobile Conductivity-Temperature-Velocity-Depth (CTVD) frame developed for the CEAREX O Camp experiment. The frame could be lowered to about 110 m depth.

be averaged before the Reynolds stress statistics "settle down."

Fig. 2a shows a 5.25-hr average (i.e., the average of 21, 15-min realizations of the Reynolds stress tensor), beginning at 103:10:08 UT, of mean velocity (relative to the ice) and Reynolds stress for three clusters on the main fixed TC frame. This may be compared with a 6-hr average starting at 103:10:15 UT of 5 clusters on the mobile CTDV frame (Fig. 2b). Although the times are not exactly the same, there is reasonably close correspondence between both velocity and turbulent stress where the depths overlap. Fig. 2c shows velocity and stress measurements from an earlier time when the mobile CTVD frame was lower in the OBL, and the flow was less energetic: the mean velocity at 22.9 m is 12.0 cm/s vs. 19.9 cm/s at 23.2 m in Fig. 2b.

The variability in stress in the upper part of the OBL, especially the decrease in stress 2 m from the interface (Fig. 2a), probably results from variation in the under-ice topography surrounding the experiment site. A side-looking sonar survey of the ice undersurface showed that the ice was relatively smooth near the deployment site, but that there here were sizable pressure ridge keels within 100 m (R. Colony, personal comm., 1989). If the roughness of the undersurface were uniform, stress would increase monotonically toward the interface; however, as the turbulence frames are usually sited under smooth ice, it is common for the stress to decrease near the surface (see, e.g., McPhee, et. al., 1987).

The profiles of Fig. 2 exhibit characteristics which distinguish these data from previous studies under sea ice.The main feature is the lack of angular shear (turning) in both vector fields. In most previous OBL measurements, the turning occurred within the upper 30 m of the water column (McPhee and Smith, 1976; McPhee, et. al., 1987); however, those data were from mixed layers that were 40 m or less thick. At the time of the present measurements, the mixed layer under O Camp was about 70 m deep (J. Morison and R. Andersen, personal comm., 1990). In order to quantify how this would affect theoretical velocity and stress profiles, we adapted a steady state, quasi-analytic OBL model (McPhee, 1990; 1991) so that it matched the modeled stress to the measured stress at a particular level (14.2 m in Fig. 3a), then reconstructed the entire stress profile, including the inferred stress at the interface, shown as the dashed vectors in Fig. 3. The model velocity profile relative to an observer on the ice was then constructed from the stress profile, with the surface layer shear specified by finding a surface roughness ($z_0 = 0.1$ m) which gave close agreement with velocity measured at the same 14.2 m depth. Results are shown in Fig. 3a, in a format chosen to facilitate comparison with the measurements. The dotted curves around the topmost vectors show theoretical hodographs (plan views) for velocity and stress for a logarithmic grid across the upper 100 m, and are included to indicate the total expected turning in both vector fields. Note that in the reference frame attached to the ice there is little angular shear in the velocity field in the upper 20 m, but that the Reynolds stress vector exhibits substantial turning.

The model includes the effect of buoyancy flux at the pycnocline on the turbulence structure, and the results show that the lack of turning in the velocity profile is not unexpected (although the angle between velocity and stress is less in the model than in the data). The modeled stress shows more turning than observed, but generally approximates a smoothed rendition of the ob-

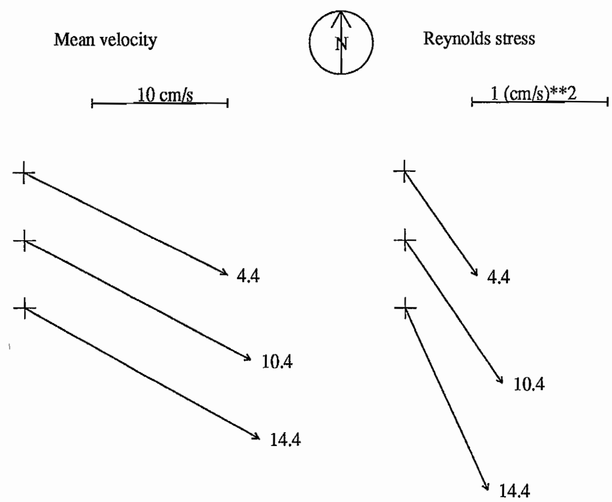

Fig. 2a. Mean velocity (relative to observer on the ice) and Reynolds stress for three clusters of the fixed frame, averaged for 5.25 hrs beginning at 103:10:14 UT. Numbers to the right of each vector are depth in m (subtract 2.4 for distance from ice underside)

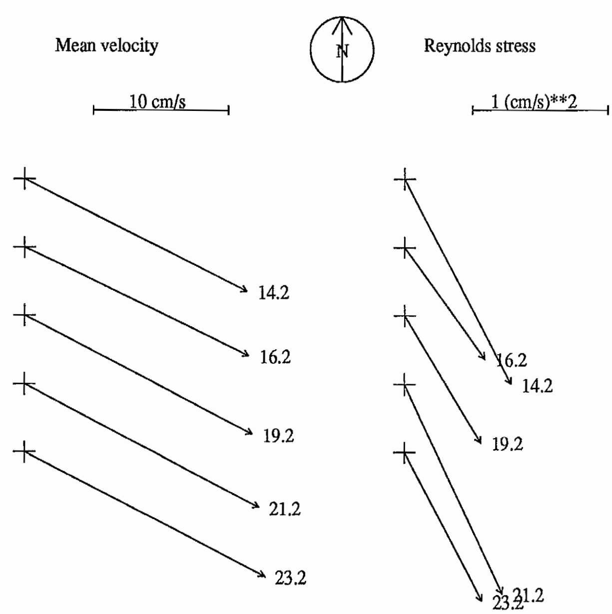

Fig. 2b. Mean velocity and Reynolds stress for the mobile CTVD frame, averaged for 6 hrs beginning at 103:10:15.

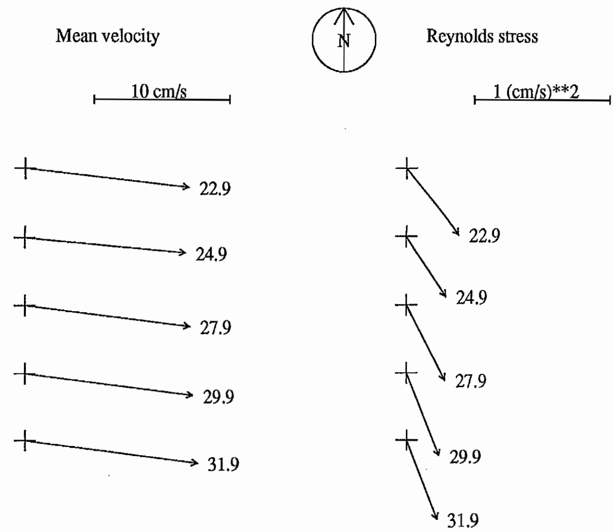

Fig. 2c. Same as Fig. 2b, except 1.75 hr average starting at 102:14:15

served stress.

For the model to have validity, it should apply as well to different conditions. This was tested by forcing the modeled stress at 22.9 m to match data from the earlier observations of Fig. 2c. Results are shown in Fig. 3b, and discrepancies are readily apparent. In order to match the observed stress at 22.9 m, the model finds a fairly high value of surface (interface) stress, which produces enough shear through the logarithmic surface layer (using the same 0.1 m for z_0) that the modeled velocity at 22.9 m is roughly 40% higher than observed. In addition, the modeled stress 9 m below the reference level is noticeably smaller and rotated farther clockwise than observed. Thus the measured velocity implies that the actual interfacial stress is smaller, and that the model overestimates attenuation of stress with depth.

While uncertainties in the model and data are large, the theoretical results suggest that stress is more uniform, and penetrates farther into, the O Camp mixed layer than we would expect based on the behavior of previously measured boundary layers. Aside from the depth of the mixed layer, a major difference between the O Camp and previous mixed layers is the strength of oceanic flow not driven directly by the wind. Recalling the discussion in Section 1, in most of the Arctic, wind is the prime mover of ice, and the *absolute* (i.e., in a frame of reference fixed to earth) velocity in the lower part of the boundary layer approaches the geostrophic current in the ocean, typically a few centimeters per second. Our impression at O Camp was that currents in the boundary layer had little

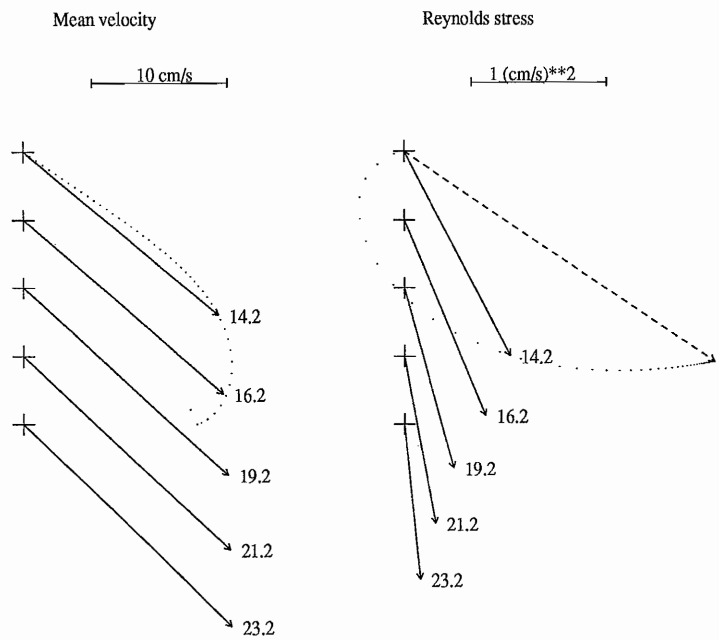

Fig. 3a. Analytic model of relative velocity and Reynolds stress, forced to match the observed stress at 14.2 m (Fig. 2b). Solid vectors are drawn offset downward to coincide with the measurement levels. The dashed stress vector is the required ice/ocean stress and hodographs of stress and velocity are shown as dotted curves emanating from the uppermost level.

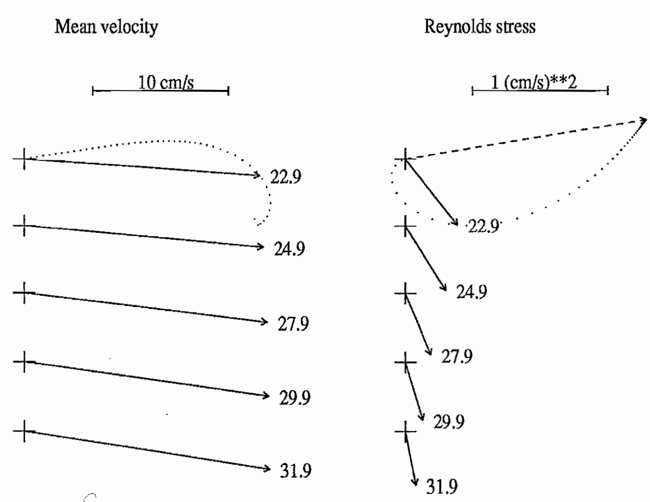

Fig. 3b. Same as Fig. 3a, except the model was forced to match the stress at 22.9 m to simulate the upper ocean structure of Fig. 2c.

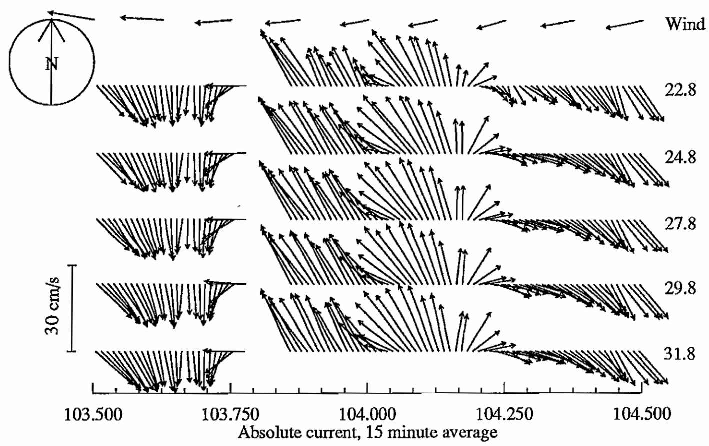

Fig. 4. Fifteen minute averages of absolute horizontal velocity at 5 levels of the mobile CTVD frame. Numbers at right indicate average depth in m. Absolute velocity is the vector sum of the measured water velocity and the ice velocity determined from satellite navigation. The row of vectors labeled "Wind" indicates surface wind velocity divided by 50, so that the scale bar at the left is equivalent to a wind magnitude of 15 m/s.

direct connection with the wind, which is substantiated by Fig. 4, showing the absolute horizontal currents at each level on the mobile frame for the period 103:12:00 to 104:12:00 UT and 3-hr averages of the surface wind. The frame was occasionally moved in the vertical during the interval shown, but remained relatively shallow until the last few hours, when it was lowered into the pycnocline. While the wind remains relatively steady from the east, there is a strong south to north and back again reversal in the flow. Shortly after midnight on day 104, there is a significant flow event superimposed on the northward part of the diurnal cycle. It may be that this energetic flow, which will be discussed further in the next section, is instrumental in increasing turbulence levels in the entire mixed layer and thus smearing the momentum exchange between the ice and ocean across a larger vertical extent.

3. Deep Boundary Layer Measurements

Results presented above are from a time with the mobile CTVD frame positioned near the surface, when it was in effect an extension of the near surface, fixed frame. Four days later, both systems measured a remarkably similar flow regime, but this time the mobile frame was near the bottom of the mixed layer. Fig. 5a shows horizontal current in the same format as Fig. 4, with the frame spanning levels from about 93 to 102 m. The deeper flow has many features of the earlier record, including the dominant diurnal reversal, a dramatic direction swing shortly after midnight, and little apparent connection with the wind. The temperature record (Fig. 5b) illustrates that strong

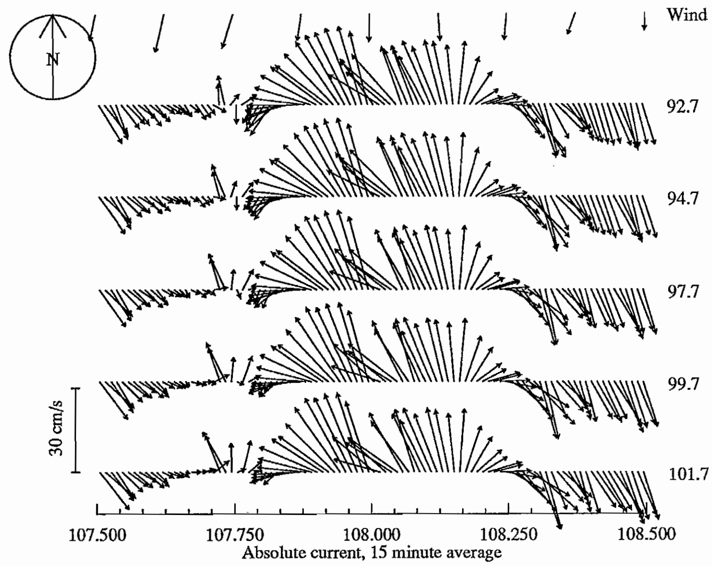

Fig. 5a. Same as Fig. 4, except for time 107:12:00 to 108:12:00, with the mobile CTVD frame deep in the mixed layer/upper pycnocline.

thermal signatures accompany both the velocity reversals and mid-cycle disturbances at intervals of slightly over 6 hrs. Salinity is not shown but follows temperature closely with a maximum excursion of about 0.4 psu. A plausible interpretation is that the recurring thermal features are some type of internal bore associated with amplification of internal tides by the Yermak Plateau to the south, as discussed in the context of a dominant diurnal component in current meter records from the region by Hunkins (1986). The disturbances are also apparent in Fig. 5c, which shows q^2 (i.e., the sum of the diagonal components of the Reynolds stress tensor), based on two-minute averages of the deviation of velocity components (measured at 1 sec intervals) from their means. The short averaging time was chosen to separate the small scale effects from variance associated with irrotational internal waves, and thus may not represent the entire turbulent spectrum; nevertheless, "patches" of intense q^2 most likely indicate active turbulent transfer down the energy cascade from larger to smaller scales. There is a period of relatively high turbulence in the afternoon of day 107 without the dramatic temperature/salinity signal, but it appears in this case that the disturbance existed deeper in the water column (L. Padman, personal comm., 1990).

The midnight event was accompanied by a packet of energetic internal waves, as illustrated most clearly in the vertical velocity records of Fig. 6. These waves were also evident in data from tiltmeters embedded in the ice (Czipott, et. al., 1990). The average spectrum of vertical velocity for the entire 24-hour period is shown in Fig. 7. Spectra were calculated for each cluster by smoothing

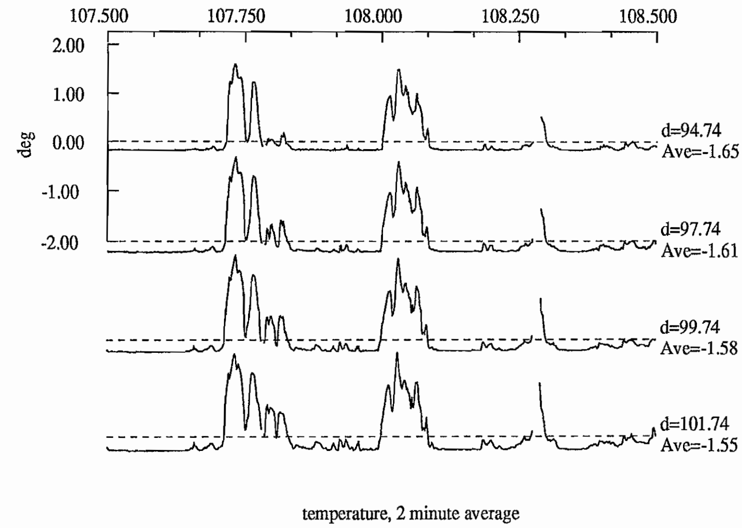

Fig. 5b. Deviations of temperature from mean values for 4 mobile frame clusters, for the period 107:12:00 to 108:12:00. Numbers at right indicate cluster depth and average temperature for the time series, in deg C.

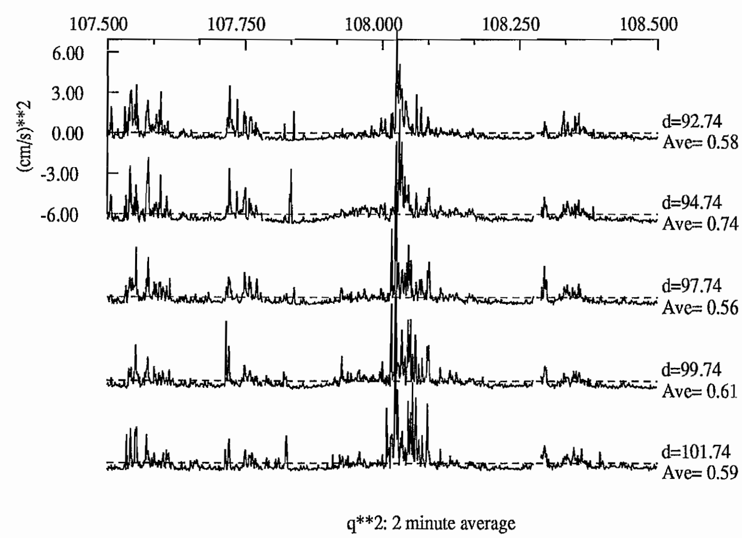

Fig. 5c. $q^2 = \langle u'u' \rangle + \langle v'v' \rangle + \langle w'w' \rangle$ averaged for two minutes, shown as deviations from the mean at 5 levels on the mobile frame.

the periodogram (proportional to the squared amplitude of the discrete Fourier transform of one minute averages of vertical velocity) with one pass of a modified Daniell filter of halfwidth 4 min^{-1} (Bloomfield, 1976). The spectra from all 5 clusters were then averaged for Fig. 7. A peak with a frequency of approximately 0.04 cpm (25 minute period) stands out, which agrees within a minute of the period reported by Czipott, et. al. (1990) in ice flexure.

A number of interesting events occur during the first 6 hrs of day 108, which may illustrate how deep mixing is enhanced in the Yermak Plateau region. A salinity profile just prior to the onset of the bore event at about midnight is shown in Fig. 8a, along with 10-min average salinities from the lower 4 clusters. The instrument frame started out near the base of the mixed layer, then apparently entered and exited the pycnocline as the interface followed the internal waves, as indicated by the difference in salinity across the instrument frame as a function of time (Fig. 8b). After the main thermal anomaly passed in about 2 hrs, the stratification reverted to its former small value. The 25-min period internal waves continued until about 05:00. The abrupt rise in q^2 lags the passage of the bore temperature front by about half an hour, then seems to die away more or less exponentially over the next 5 hrs. A picture thus emerges of an internal bore, which is itself highly turbulent, traversing the lower part of the mixed layer, leaving energetic internal waves and elevated turbulence levels in its wake.

A detail of the spectra of vertical velocity for the first 6 hrs of day 108 is shown in Fig. 9. The solid line is the average spectrum for the upper three clusters on the mobile frame, with symbols indicating individual spectra for the same three clusters (the lower two clusters are not shown in order to keep the graph legible, but are quite similar to cluster 3, marked by pluses). Near the 25-minute peak [log(f)= -1.4], there is a substantial difference in energy density across the 5 m span of the clusters. There is a plateau in the frequency range from log(f)= -1.1 (1/12 min) to -0.8 (1/6 min) which may indicate harmonics of the dominant internal waves, or the dominant turbulent eddy size, or perhaps a combination of both. At the higher frequencies, the energy levels of the higher cluster (asterisks) are no longer discernibly smaller, in fact may be larger.

Similar velocity measurements are available from two, 3-hr records of the fixed-mast turbulence system near the surface, spanning the period from 107:23:56 to 108:06:14. Fig. 10 shows power spectra of 1-min averages of vertical velocity for clusters at 4, 8, and 12 m below the ice/water interface in the same format and to the same scale as Fig. 9. Calculation of the spectra is the same as before, except that the individual cluster spectra are the average of spectra from two 3-hr segments instead of one 6-hr segment. There is essentially no indication in the shallower data of the 25-min waves, even 12 m below the ice. In fact, the spectra begin to fall off near the peak of the lower spectra. This was somewhat surprising in view of the tiltmeter results mentioned above; on the other hand, the actual displacement of the ice is very small, and if there is energy at 25 min, it is masked by the turbulence levels at higher frequencies. The lack of a spectral peak in the cluster at 12 m is important because it shows that the 25-min waves are not losing their energy only when they encounter the high stress and shear near the interface, but that much of the energy transfer to turbulence is happening near the base of the mixed layer.

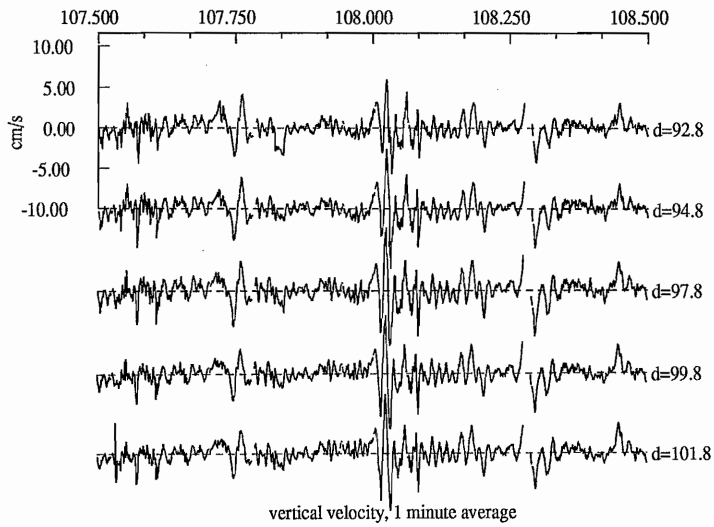

Fig. 6. Time series of vertical velocity at 5 levels on the mobile frame. Each small time division is 2 hrs.

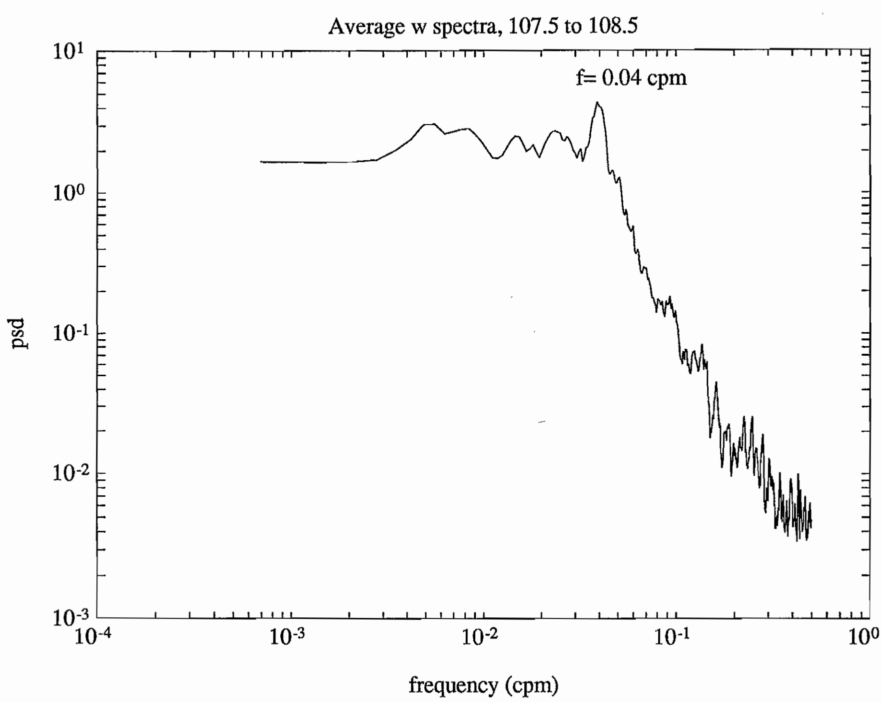

Fig. 7. Average power spectrum of vertical velocity for 5 clusters of the mobile frame for the period 107:12:00 to 108:12:00 UT. Spectra for each cluster are calculated by smoothing the periodogram of 1-min velocity averages with one pass of a modified Daniell filter of halfwidth 4 min^{-1}.

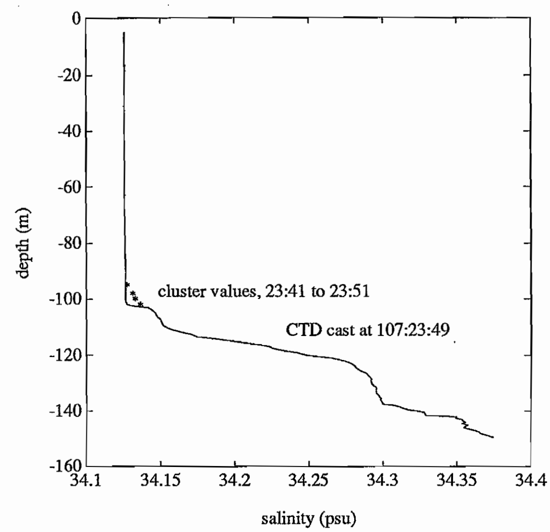

Fig. 8a. Salinity profile (courtesy J. Morison and R. Andersen) just prior to the onset of the anomalous event starting at midnight. Asterisks mark the 10-min average of mobile frame salinities at approximately the same time.

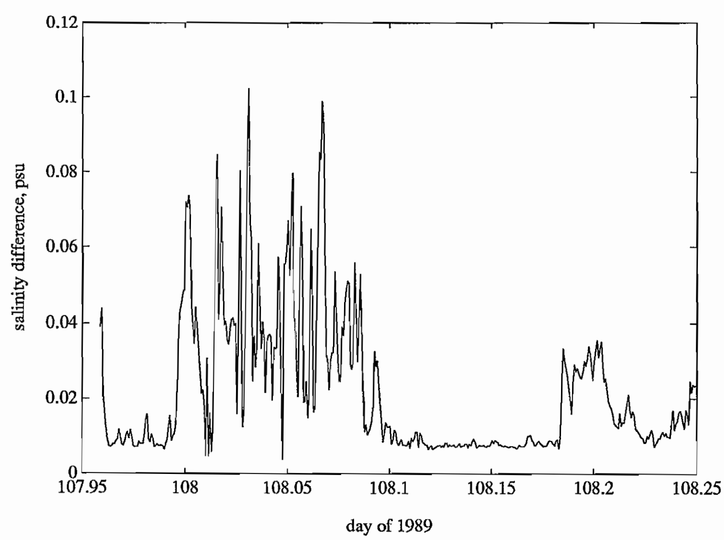

Fig. 8b. Time series of the difference in salinities between mobile frame cluster 4 (at 101.7 m) and cluster 2 (at 94.7 m) for the period 107:23:00 to 108:06:00 UT.

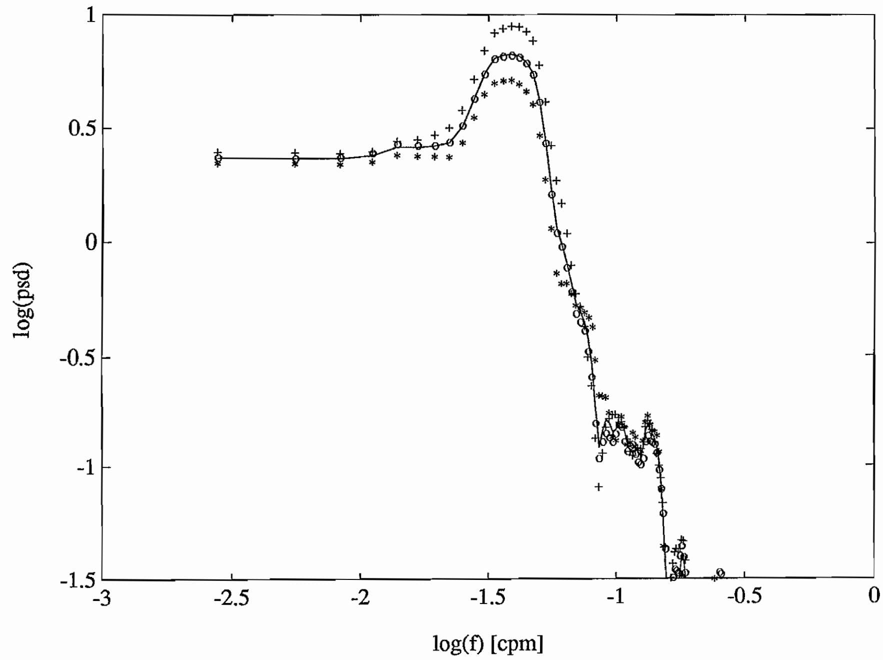

Fig. 9. Power spectra of vertical velocity from three clusters on the mobile frame for the period 108:00:00 to 108:06:00. Symbols mark spectra from individual clusters: cluster 1 at 92.7 m (*), cluster 2 at 94.7m (o), and cluster 3 at 97.7 m (+). The solid curve is the average. Spectra from deeper clusters are similar to cluster 3.

A reasonable interpretation of the spectra of vertical velocity from both deep in the mixed layer and near the surface, is that energetic internal waves are propagating into the system from below, and losing their energy as they encounter the low stability and existing turbulence in the lower part of the mixed layer. Fig. 9 is provocative in that if it truly represents a transfer of energy from the frequency of the dominant internal waves to smaller scales across the 5 m separation of the three clusters, then it shows that the main source of TKE just above the main pycnocline comes from below.

4. Summary

While the upper ocean under O Camp was never close to overturn and subsequent deep convection, the regime there may be the closest Arctic analog yet studied of the ice covered winter mixed layer of the Weddell Gyre, where overturn is possible with slight variation of the forcing parameters (Martinson, this volume). The question posed for each region is how the upper ocean remains mixed to deep levels (by polar standards) when destabilizing surface buoyancy is cut off by the ice cover, and when upwelling and diffusion across the pycnocline tend to reduce the mixed layer depth. Results of the present study suggest that activity in the pycnocline below the mixed layer may have significant impact on the turbulence and momentum flux in the OBL. A source of OBL turbulence other than direct shear at the ice/ocean interface would mimic some aspects of an unsta-

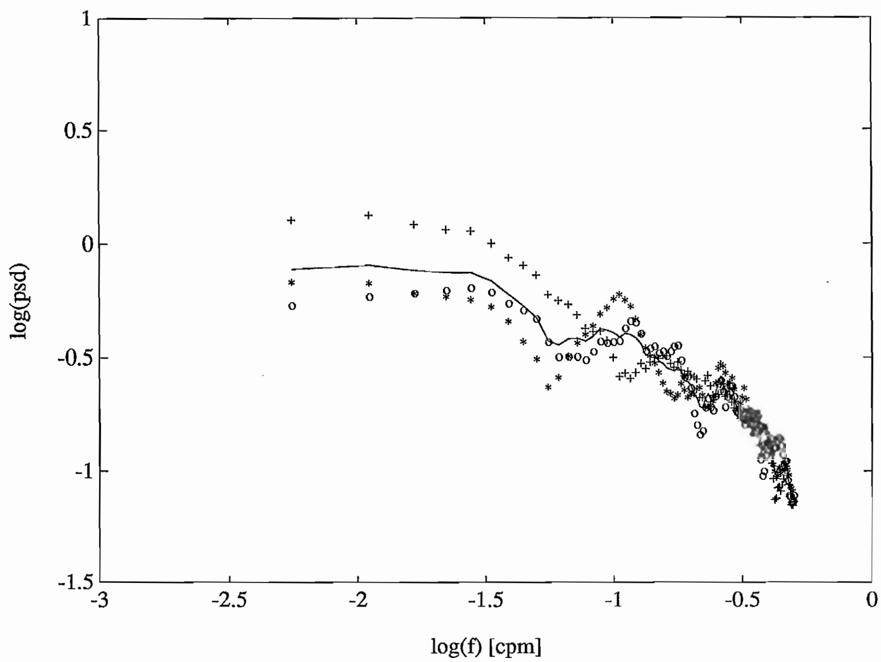

Fig. 10. Power spectra of vertical velocity from three clusters on the main fixed frame for the period 107:23:56 to 108:06:14. The format, including plot scales for direct comparison, is the same as Fig. 9, except: cluster 1 at 6.4 m (4 m below the ice) (*); cluster 2 at 10. 4 m (o); cluster 3 at 14.4 m (+). Note the lack of a discernible peak at 25 min [log(f)= -1.4].

ble, convective boundary layer: i.e., just as stable stratification reduces the size of turbulent eddies, and confines the OBL momentum (deficit, in this case) to smaller depths with more angular shear (see, e.g., McPhee, 1983; Mellor, et.al., 1986), an agent that increases eddy size would conversely increase the scale of the OBL and reduce the turning. The near surface measurements in Section 2 showed that stress levels were higher in the range from 15-30 m than we had come to expect from previous studies of neutral boundary layers under sea ice, implying some enhancement of turbulence levels. The ice cover in the vicinity of O Camp was relatively thick and compact, thus it is unlikely that unstable buoyancy flux had much influence on OBL dynamics.

A case study of an energetic packet of internal waves superimposed on what appears to be a fairly regular tidal bore that traverses the O Camp region, may indicate where the enhanced turbulence originates. Fig. 5c shows that small scale velocity fluctuations (most likely turbulence) near the base of the mixed layer are strongly intermittent and related to the larger scale flow features. Fig. 9 shows a steep vertical gradient in power spectral density in the vertical velocity components near the mixed layer/pycnocline interface. The vertical displacement associated with a simple internal wave with the vertical velocity amplitude observed shortly after midnight on day 108 (Fig. 6) is about 20 m, yet 80 m higher in the boundary layer (and still 12 m from the interface), there was virtually no evidence of the 25-min waves in the vertical velocity spectrum (Fig. 10). The clear implication is that quite a lot of energy has been transferred from lower to higher wavenumber scales, and that as the internal waves impinge on the mixed layer from below, the process takes place preferentially at depth. A source of turbulence for maintaining a sharp interface deep in the mixed layer is thus identified.

What created the oceanic conditions responsible for the activity below the OBL at O Camp is beyond the scope of this work, yet it may be germane to point out the geometric similarities between the Arctic Ocean floor around the Yermak Plateau, and the Weddell Sea in the vicinity of Maud Rise. While the proximity of Maud Rise to the initial location of the Weddell Polynya of the 1970s may be coincidental, one can speculate that an increase in internal wave activity in the pycnocline, say from the interaction of an oceanic eddy with Maud Rise, might have raised turbulence levels in the mixed layer, and entrainment at its base, enough to initiate deep convection, and then to prevent re-establishment of the stable winter regime now dominant. Further research, both observational and theoretical, seems warranted.

5. Acknowledgment

Support for this work by the Office of Naval Research, Contract N00014-84-C-0028 is gratefully acknowledged, as is help in the field from the CEAREX logistics staff and fellow O Camp scientists. I thank R. Andersen, K. Davidson, P. Guest, and J. Morison for providing data. Comments on the manuscript by P. Czipott, L. Padman, and an anonymous reviewer are appreciated.

6. References

Bloomfield, P. 1976. *Fourier Analysis of Time Series: An Introduction.* John Wiley and Sons, New York, 258 pp.

Czipott, P.V., W. Podney, M.D. Levine, C.A. Paulson, and R. Williams. 1990. Ice flexure forced by an internal wave packet in the Arctic Ocean. *Eos, Transactions of the Am. Geophys. Union, 71,* p. 130 (abstract).

Guest, P.S., and K.L. Davidson. 1989. CEAREX "O" and "A" Camp meteorology atlas, Naval Postgraduate School data report (unpubl.), Monterey, CA

Gordon, A.L., and B. Huber. 1990. Southern Ocean winter mixed layer, *J. Geophys. Res. 95,* 11,655-11,672.

Hunkins, K. 1986. Anomalous diurnal tidal currents on the Yermak Plateau, *J. Mar. Res., 44,* 51-69.

McPhee, M.G. 1990. Small scale processes, in: *Polar Oceanography,* ed. W. Smith, 287-334, Academic Press, San Diego, CA.

McPhee, M.G. 1991. A quasi-analytic model for the under-ice boundary layer, in press, *Annals of Glaciology.*

McPhee, M.G., G.A. Maykut, and J.H. Morison, 1987. Dynamics and thermodynamics of the ice/upper ocean system in the marginal ice zone of the Greenland Sea. *J. Geophys. Res., 92,* 7017-7031.

McPhee, M.G., and J.D. Smith. 1976. Measurements of the turbulent boundary layer under pack ice, *J. Phys. Oceanogr., 6,* 696-711.

McPhee, M.G., and N. Untersteiner, 1982. Using sea ice to measure vertical heat flux in the ocean. *J. Geophys. Res., 87,* 2071-2074.

Martinson, D.G. 1990. Evolution of the Southern Ocean winter mixed layer and sea ice: Open ocean deepwater formation and ventilation. *J. Geophys. Res. 95,* 11,641-11,654.

Mellor, G.M., M.G. McPhee, and M. Steele. 1986. Ice-seawater turbulent boundary layer interaction with melting or freezing. *J. Phys. Oceanogr., 16,* 1829-1846.